An Atlas of STIS-HST spectra of Seyfert Galaxies

P. F. Spinelli, T. Storchi-Bergmann, C. H. Brandt

Instituto de Física, UFRGS, Porto Alegre, RS, Brazil

patricia.spinelli@ufrgs.br

and

D. Calzetti

Space Telescope Science Institute, Baltimore, MD 21218

Received _____; accepted _____

ABSTRACT

We present a compilation of spectra of 101 Seyfert galaxies obtained with the Space Telescope Imaging Spectrograph (HST-STIS), covering the UV and/or optical spectral range. Information on all the available spectra have been collected in a *Mastertable*, which is a very useful tool for anyone interested in a quick glance at the existent STIS spectra for Seyfert galaxies in the HST archive, and it can be recovered electronically at the URL address **www.if.ufrgs.br/~pat/atlas.htm**. Nuclear spectra of the galaxies have been extracted in windows of $0\farcs2$ for an optimized sampling (as this is the slit width in most cases), and combined in order to improve the signal-to-noise ratio and provide the widest possible wavelength coverage. These combined spectra are also available electronically.

1. Introduction

Spectra obtained with the Space Telescope Imaging Spectrograph (HST-STIS) provide unique information on the spectral energy distribution (SED) of active galactic nuclei (AGN), in two aspects: the coverage of the ultraviolet spectral range, which is not observable from the ground, and the high angular resolution which enhances the contrast between the nuclear continuum and that of the stars of the host galaxies. Now that STIS has ceased to work, it is timely to compile the data accumulated by observations with this instrument in an Atlas. In the present work we provide such compilation for 101 Seyfert galaxies.

We have used the spectra to construct nuclear SED's of Seyfert galaxies obtained from extractions at an optimized sampling, corresponding to an aperture $0\farcs2 \times 0\farcs2$, as $0\farcs2$ is the width of the slit in most observations. These combined nuclear spectra are available

electronically, and can be used for a number of studies. The small extraction window allows us to better isolate the nuclear SED, minimizing the contamination by the bulge of the host galaxies. These spectra can be compared with data obtained through large apertures using ground based telescopes in order to evaluate the contribution of the of host galaxies, particularly useful when studying samples of distant AGNs. These spectra can also be used to investigate the contribution of other sources very close to the nucleus, such as starbursts (Storchi-Bergmann et al. 2005; González Delgado et al. 2004).

Although the HST archive provides one-dimensional spectra, which are identified by the terminations *_x1d* and *_sx1*, our Atlas has at least three advantages:

(1) The *_x1d* and *_sx1* are obtained with a extraction window of 11 pixels for the UV corresponding to 0.″27, and 7 pixels for the optical – corresponding to 0.″35. Therefore, the extraction windows in the UV an optical are different and do not make optimal use the angular resolution provided by HST. Our extraction window is chosen to have the same angular extent of the slit width, 0.″2 in all wavelength ranges, providing spectra with better angular resolution. For AGN, a smaller extraction window increases the contrast between the active nucleus and the host galaxy.

(2) In many cases the HST pipeline does not perform averages of spectra. This is the case of the *_x1d* spectra which are very noisy.

(3) The pipeline also does not "glue" the different spectral segments together. In the Atlas we have done this after eliminating the noisy borders of each spectral segment.

Our Atlas thus provides better signal-to-noise ratio nuclear spectra with the widest available spectral coverage, with the different spectral ranges already combined and edited to eliminate the noise usually present at the initial and final wavelengths of each segment.

In the process of constructing the Atlas, we have compiled relevant information on all

the available spectra we have been collected in in a *Mastertable*. It contains for example, initial and final wavelengths of the different spectra segments, exposure times, gratings and slit width. This *Mastertable* is by itself a very useful tool for anyone interested in a quick glance at the available STIS spectra for Seyfert galaxies in the HST archive and can be recovered electronically as the spectra.

This paper is organized as follow: section 2 describes our sample selection. Section 3 presents the *Mastertable* and describes the information contained in it. The extraction of the spectra is described in section 4 and their combination is explained in section 5. The results and some potencial applications are discussed in section 6.

2. Sample and Data

The sample was initially selected as all Seyfert galaxies listed in the catalog of Véron-Cetty & Véron (1996) with redshift $z \leq 0.03$, which had STIS spectra available in the archive. We have later tried to incorporate the remaining Seyfert galaxies ($z \geq 0.03$). Misclassification, however, may have prevented a comprehensive inclusion of all Seyfert galaxies in the HST archive. Thus our sample comprises most galaxies (101 in the total) classified as Seyfert with available STIS spectra in the HST archive until September 2004. Although the most valuable wavelength range is the UV because it is not accessible from the ground, we have included in the Atlas also those cases in which only optical spectra were available. The sample galaxies are listed in Table 1, which contains information on the positions, Hubble type, activity type, redshift and references to previous works in which the spectra have been used. The seventh column of Table 1 gives the spectral coverage (in the observed frame) of the resulting nuclear spectrum after the individual extractions and combination of the different spectral segments.

3. The Mastertable

Relevant information about all the two-dimensional (hereafter 2-D) spectra collected is summarized in a *Mastertable*, available electronically in the URL address **www.if.ufrgs.br/~pat/atlas.htm**. The columns of the table contain the following information: (1) the name of the galaxy; (2) the identification of all available STIS spectra for this galaxy in the HST archive, one per line; (3) the grating used in each observation; (4) the slit width of each observation; (5) the central wavelength (in the observed frame); (6) the initial wavelength (in the observed frame); (7) the final wavelength (in the observed frame); (8) the spectral resolution; (9) the slit orientation; (10) the exposure time. In column (11) we list the identification of the extracted spectrum from each segment, which will be useful in a few cases in which we could not combine the spectra of the same galaxy (for example, because they were obtained in different slit positions) and we then provide the individual extracted spectra without combining them. These spectra are identified according to following convention: compact name of the galaxy followed by an arbitrary ordering number and the slit orientation. For example, n3516-13.97 means the 13th spectrum of the galaxy NGC 3516 which was obtained at slit orientation of 97 degrees. Finally, in column (12) we list the platescale of the observations. In Table 2 we present a printout of a few selected lines of the *Mastertable* (which has 1001 lines), for illustrative purposes.

4. Extraction of the spectra

The nuclear spectra were obtained from 2-D reduced STIS spectra, which have been rectified, wavelength and flux calibrated, and are identified in the HST archive by the suffixes *_x2d* and *_sx2*. The latter are summed *_x2d* spectra (when the observations were performed in the *cr-split* or *repeatobs modes*). When both *_x2d* and *_sx2* spectra were

available, we used the latter.

One-dimensional (hereafter 1-D) spectra were extracted from the 2-D spectra in windows of 0.″2 from a long-slit spectrum usually obtained through a slit width 0.″2 and covering 52″ in the sky. The *IRAF* task *apall* was used to perform the extractions. We performed the sky subtraction by fitting a straight line to regions along the slit with no (or negligible) galaxy contribution. For each galaxy, different sky windows were defined, in order to avoid including contribution from the galaxy. The sky level was always negligible, except in the Lyman alpha Geocoronal emission line.

Although the redshift range for the sample is $0 \leq z \leq 0.37$, only for 15% of the galaxies $z \geq 0.06$, such that the 0.″2 aperture corresponds at the galaxies to more than 200 pc. For 60% of the sample, 0.″2 corresponds to < 60 pc at the galaxies, while for 30% of the sample it corresponds to < 20 pc. We are thus sampling a very small region around the active nucleus, providing the best possible contrast between the AGN and galaxy bulge.

We extracted only nuclear spectra which we identified as being centered at the peak of the continuum flux along the slit. This was done by inspecting the spatial light distribution in a spectral region devoid of emission or strong absorption lines (the continuum) and centering the extraction window at the peak of the continuum flux distribution. In a few cases the 2-D spectra contained only emission-lines, with no continuum. In these cases, for which we could not identify a continuum source we did not extract the spectra, but the information on the available 2-D spectra are still listed in the *Mastertable*, with a cautionary note explaining why the spectra have not been extracted.

In the cases for which there were more than one continuum source we extracted the brightest one. Although we cannot be absolutely sure for all cases, Seyfert galaxies are usually the brightest object. There are two exceptions, for which we did not extract the spectra because the two sources were equally bright. These two cases have also been

identified in the *Mastertable* with a cautionary note.

After extracting the spectra, for the galaxies which had more than one exposure for each spectral range (and with the same spectral resolution, orientation and plate scale), we constructed averages to improve the signal-to-noise ratio, eliminating also cosmic-rays and other defects when detected. The average was only constructed after checking also if the spectra had similar flux level. For the construction of the average spectra we have used the task *scombine* in IRAF, with the rejection algorithm *avsigclip* when three or more spectra were available or *minmax* when there were only two spectra. This step is illustrated in Fig. 1.

5. Combination of the spectra

The final spectra were obtained by combining the data from the different spectral ranges using the same task *scombine* in IRAF, after editing out noisy regions at the borders of each spectral segment, and checking that there were no significant differences between their fluxes. We did not find such differences for most of the cases in which there was a significant superposition of adjacent spectral segments. This final step is illustrated in Fig. 2.

In the case of the Seyfert 1 galaxies there is the issue of variability, so that spectra obtained in different dates may show different fluxes, in line and continua. We have checked the dates and found only five cases of Seyfert 1 galaxies with spectral segments obtained in different dates: NGC 4151, NGC 4258, PKS 1739+184 and AKN 564. In the case of IRAS 13224-3809, 2 of the combined 7 spectra were obtained one day latter than the other 5, thus the effect of variability should be minimal. We have identified these cases with a note in Table 1 and in the *Mastertable*. Nevertheless, we did not find any obvious

discrepancy in fluxes when combining the different spectral segments of these galaxies.

Finally, we would like to point out that, prior to the extraction, the flux units were $erg\,s^{-1}\,\mathrm{cm}^{-2}\,\text{Å}^{-1}\,\mathrm{arcsec}^{-2}$ (see STIS Data Handbook). When we performed the extraction with *apall* to sum over a few pixels (0.″2 aperture) along the slit direction, the extracted spectrum is in units equivalent to $pixel \times erg\,s^{-1}\,\mathrm{cm}^{-2}\,\text{Å}^{-1}\,\mathrm{arcsec}^{-2}$. Then, in order to consistently provide the flux integrated in the extraction window, in units of $erg\,s^{-1}\,\mathrm{cm}^{-2}\,\text{Å}^{-1}$, we multiplied each segment by a factor which is the product of the slit width and plate scale. For example, for one segment with a slit width of 0.″2 and platescale 0.″024 $pixel^{-1}$, the factor is $0.0048\,arcsec^{-2}\,pixel^{-1}$. For another segment with platescale 0.″05 $pixel^{-1}$, with the same slit width, the factor is $0.01\,arcsec^{-2}\,pixel^{-1}$.

6. Results

The combined spectra presenting the largest spectral coverage are shown in Figs. 3 and 4. There are only 9 galaxies for which we could obtain the complete STIS UV-optical spectral coverage (∼1000–10000Å).

In Figs. 5, 6 and 7 we show the redshift corrected spectra for the galaxies with UV coverage in the 1100–1600Å wavelength range, useful for looking for signatures of starbursts. In order to do that, we have drawn in the figures vertical lines at the locations of the absorption features characteristic of starbursts. While most lines are interstellar, we identify by asterisks the ones which originate in the atmosphere of young stars (Kinney et al. 1993; Vazquez et al. 2004), which are C III λ1175.65, N V $\lambda\lambda$1238.81, 1242.80, C II $\lambda\lambda$1334.53, 1335.70, Si IV $\lambda\lambda$1393.76, 1402.77, and C IV $\lambda\lambda$1548.20, 1550.77. Both the interstellar and stellar features of a starburst have been found in the UV spectrum of NGC 1097, as pointed out by Storchi-Bergmann et al. (2005). Figure 5 shows that the same

features seem to be present in the spectrum of NGC 3227, suggesting that, also in this case, as in NGC 1097, there is a starburst closer than 8 pc from the nucleus in NGC 3227 (the distance at the galaxy corresponding to 0.″1 the angular distance from the nucleus covered by the aperture of the nuclear extraction). Indeed, the presence of traces of young stellar population in an optical nuclear spectrum of NGC 3227 have been previously reported by González Delgado & Perez (1997). These features seem also to be present in the spectrum of NGC 4151, but this has to be investigated further, as they may be due to absorptions in our galaxy, due to the proximity of NGC 4151. An obvious case of interstellar absorptions from our galaxy can be observed in the UV spectrum of NGC 3516 (Fig. 5), where absorptions from O I λ1302.08 + Si II λ1304.40 and C II $\lambda\lambda$1334.53,1335.70 originating in the Milky Way appear blueshifted from their wavelengths due to the shift of the spectrum to the rest frame of the galaxy.

All spectra are available electronically at the URL address: **www.if.ufrgs.br/~pat/atlas.htm**, where they can be visualized and recovered by clicking on the name of the galaxy. We also make available at the above address the *Mastertable*, which has a compilation of the relevant information on each spectrum used in the combination.

Finally, we point out that there are several spectra which were obtained only with the highest resolution gratings, therefore covering a short wavelength range. In many cases there is also a sequence of such spectra obtained at adjacent slit positions, apparently for kinematic studies. In these cases, we did not combine the spectra but provide instead the individual extractions in a *tar* file.

REFERENCES

Barth, A. J. et al. 2001, ApJ, 555, 685B

Barth, A. J. et al. 2001, ApJ, 546, 205B

Bellamy, M. J. & Tadhunter, C. N. 2004, MNRAS, 353, 105B

Bowen, D. V. 2002, ApJ, 580, 169B

Bradley, L. D., Kaiser, M. E., Baan, W. A. 2004, ApJ, 603, 463B

Cappellari, M. et al. 2002, ApJ, 578, 787C

Capetti, A., Marconi, A., Macchetto, D. & Axon, D. 2005, å, 431, 465

Cecil, G. et al. 2002, ApJ, 568, 627C

Chandar, R., Ford, H. C. & Tsvetanov, Z. 2001, AJ, 122, 1330C

Chandar, R., Ford, H. C. & Tsvetanov, Z. 2001, AJ, 122, 1342C

Colina, L., González Delgado, R., Mas-Hesse, J. M. & Leitherer, C. 2002, ApJ, 579, 545C

Collier, S. et al. 2001, ApJ, 561, 146C

Collins, N. R. et al. 2005, ApJ, 619, 116C

Crenshaw, D. M. et al. 2000, ApJ, 545, 27C

Crenshaw, D. M. et al. 2001, ApJ, 555, 633C

Crenshaw, D. M. et al. 2002, ApJ, 566, 187C

Edelson, R. 2000, ApJ, 534, 180E

Farrah, D. et al. 2005, ApJ, 626 70F

Ferruit, P. et al. 2004, MNRAS, 352, 1180F

González Delgado, R. M. & Perez, E. 1997, MNRAS, 284, 931

González Delgado, R. et al. 2004, ApJ, 65, 127

Ho, L. C. et al. 2002, PASP, 114, 137H

Hughes, M. A. et al. 2003, AJ, 126, 742H

Hughes, M. A. et al. 2005, AJ, 130, 73H

Hutchings, J. B. et al. 1998, AJ, 116, 634H

Hutchings, J. B. et al. 1999, AJ, 118, 2101H

Hutchings, J. B. et al. 2002, AJ, 124, 2543H

Jenkins, E. B. et al. 2003. AJ, 125, 2824J

Kaiser, M. E. et al. 2000, ApJ, 528, 260K

Kinney, A., Bohlin, R. C., Calzetti, D., Panagia, N., & Wuse, R. F. G. 1993, ApJS, 86, 5

Kraemer, S. B. et al. 2000, ApJ, 531, 278K

Kraemer, S. B. et al. 2000, ApJ, 544, 763K

Kraemer, S. B. et al. 2001, ApJ, 551, 371K

Leighly, K. M. 2004, ApJ, 611, 125L

Leighly, K. M., Moore, J. R. 2004, ApJ, 611, 107L

Nelson, C. H. 2000, ApJ, 531, 257N

O'Dea, C. et al. 2003, PASA, 20, 80

Penton, S. V., Stocke, J. T. & Shull, J. M. 2004 ApJS, 152, 29P

Pogge, R., Fields, D. L., Martini, P. & Shields, J. 2003, in Active Galactic Nuclei: from Central Engine to Host Galaxies, eds. S. Collin, F. Combes & I. Schlosman, ASP Conf. Ser., Vol. 290, p. 239.

Romano, P. et al. 2004, ApJ, 604, 635R

Ruiz, JosR. et al. 2001, AJ, 122, 296

Sabra, B. M. et al. 2003, ApJ, 584, 164S

Sarzi, M. et al. 2001, ApJ, 550, 65S

Sarzi, M. et al. 2002, ApJ, 567, 237S

Sarzi, M. et al. 2005, ApJ, 628, 169S

Storchi-Bergmann, T. et al. 2005, ApJ, 624, L13

Tadhunter, C. et al. 2003, MNRAS, 342, 861T

Véron-Cetty, M. P. & Veron, P. 1996, ESO Scientific Report, Garching: European Southern Observatory, 7th ed.

Vazquez, G. A., et al. 2004, ApJ, 600, 162

Whittle, M., Rosario, D. J., Silverman, J. D., Nelson, C. H. & Wilson, A. S. 2005, AJ, 129, 104W

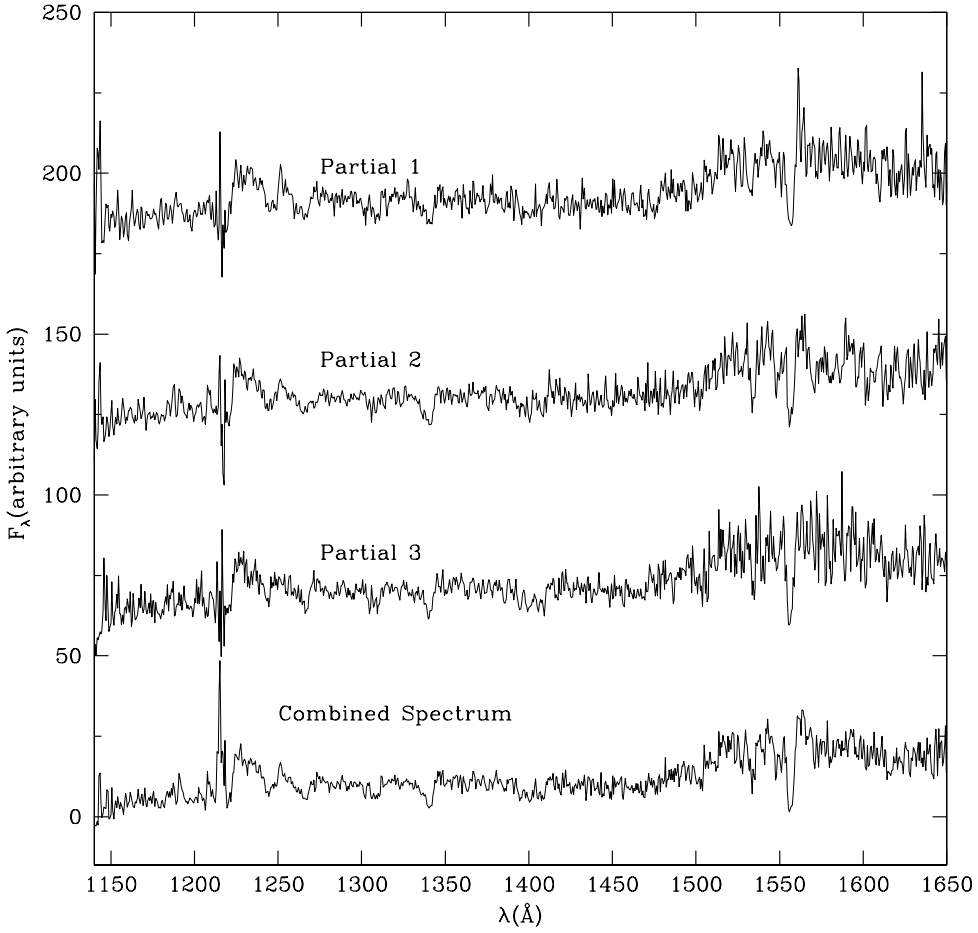

Fig. 1.— Illustration of the process of averaging three UV spectra (observed frame) of the galaxy NGC 1097.

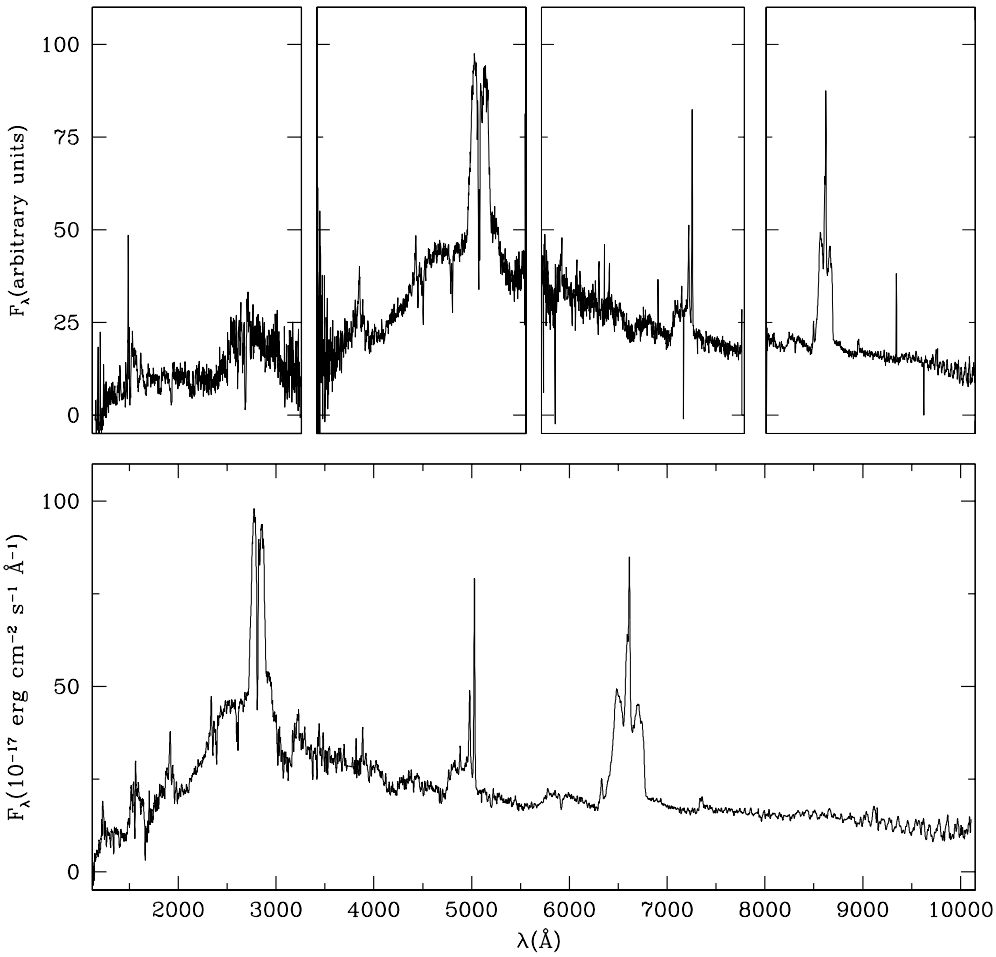

Fig. 2.— Illustration of the process of combining different spectral segments (observed frames) for the galaxy NGC 1097.

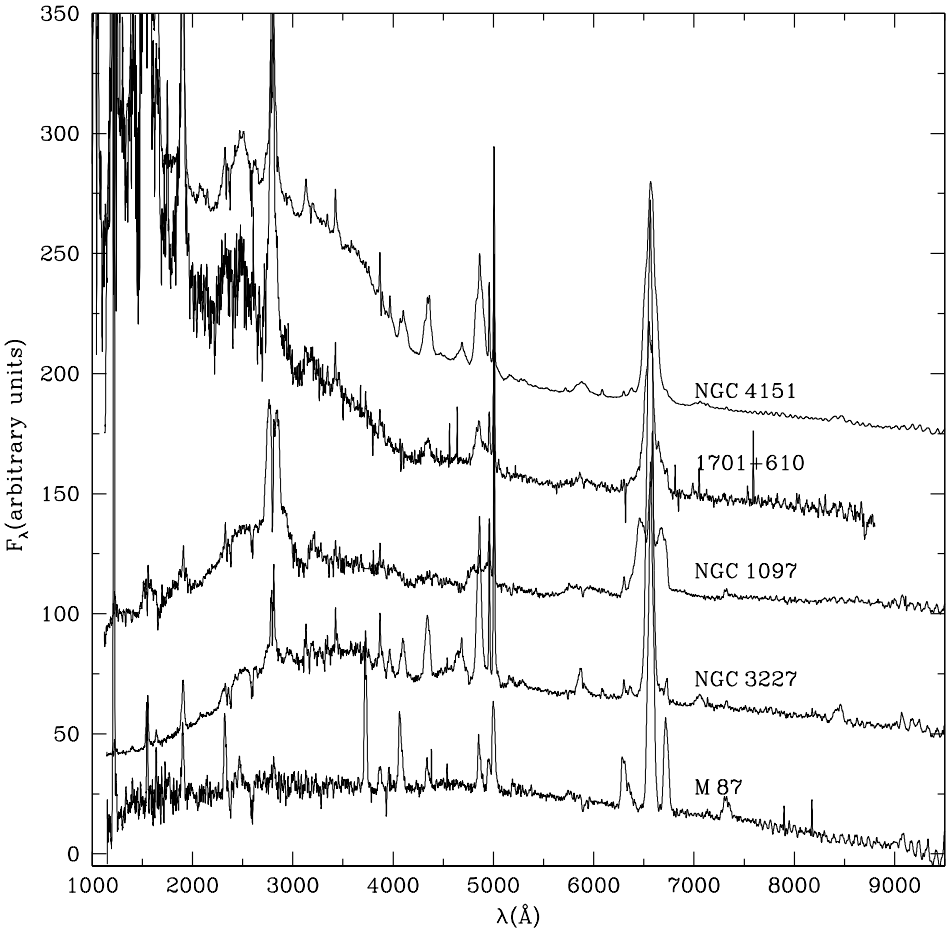

Fig. 3.— Illustration of 5 of the 9 spectra with widest spectral coverage, The spectra have been shifted to the rest frame of the galaxies.

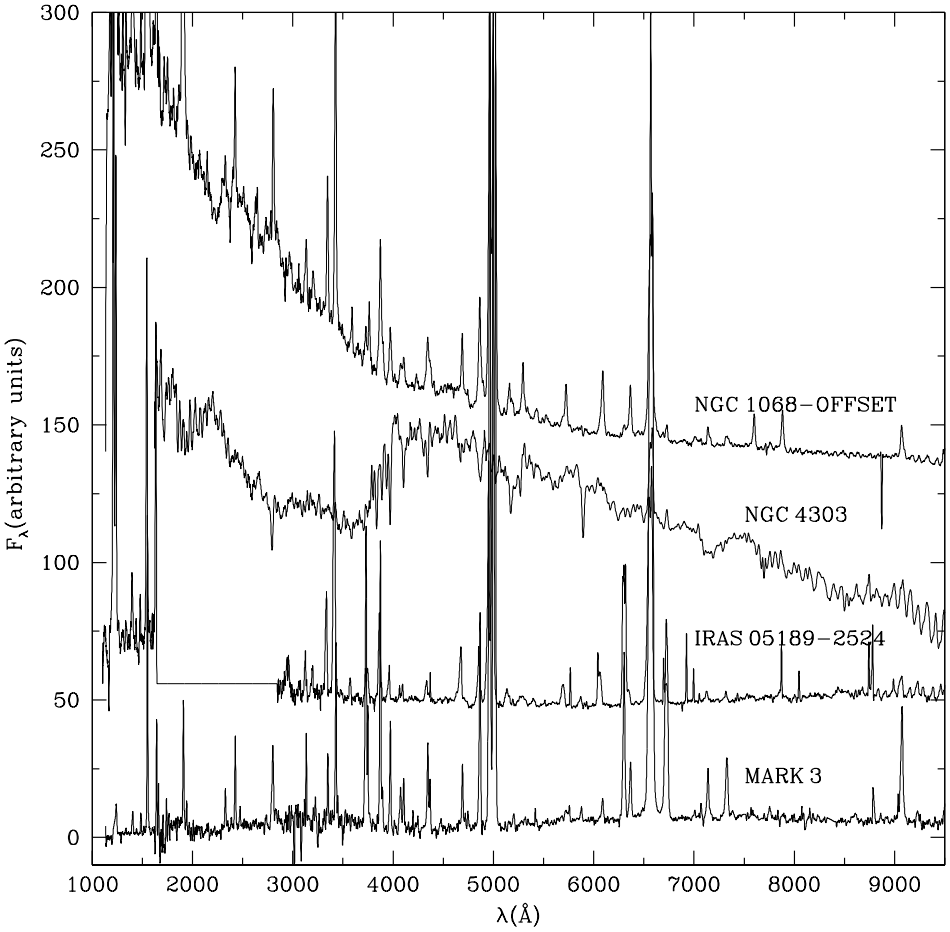

Fig. 4.— Same as Fig. 3 for another 4 spectra.

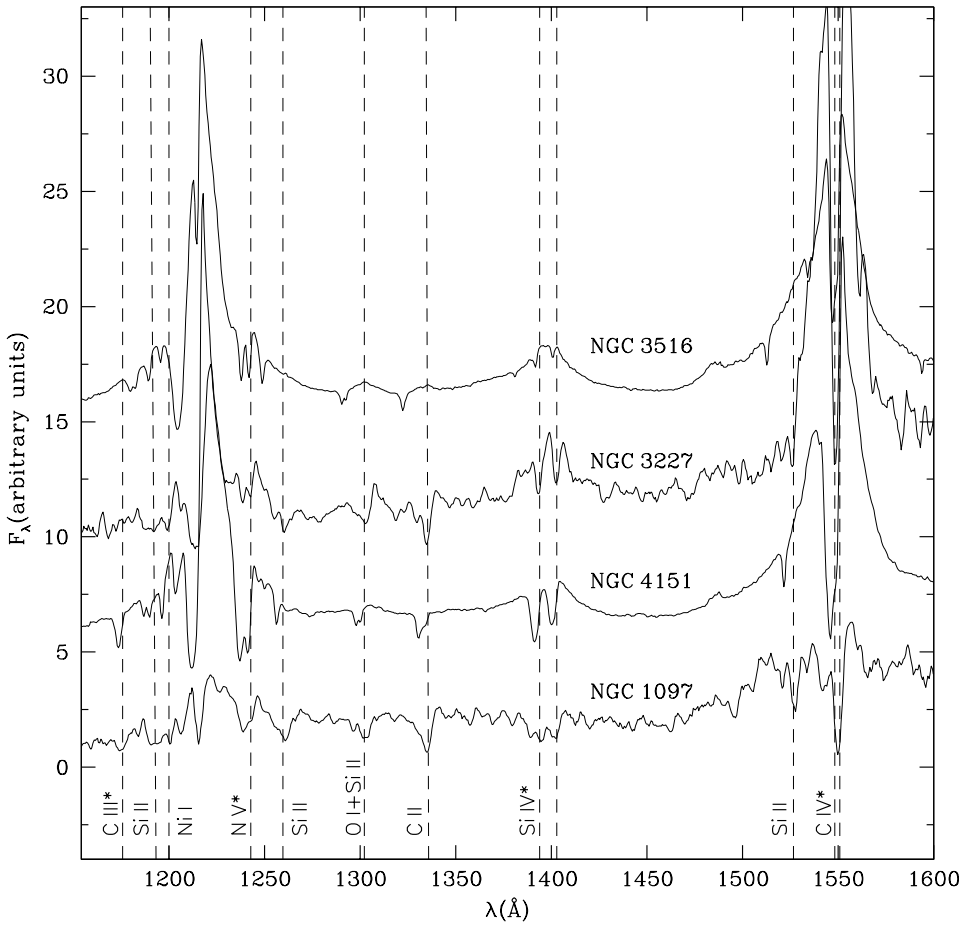

Fig. 5.— Illustration of 4 of the 12 spectra with UV coverage in the 1100–1600Å wavelength range. The spectra have been shifted to the rest frame of the galaxies. The vertical dashed lines show the location of absorption features typical of starbursts. Asterisks identify the absorption lines which originate in the atmosphere of early-type stars.

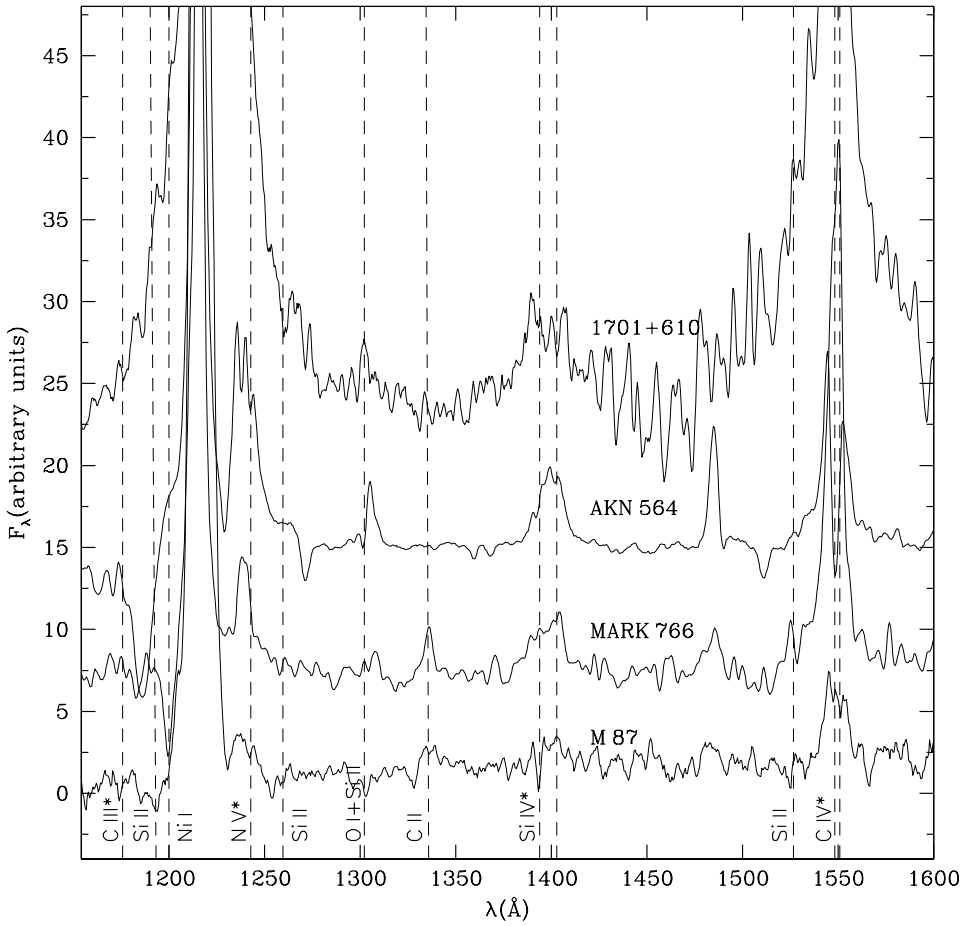

Fig. 6.— Same as Fig. 5 for another 4 spectra.

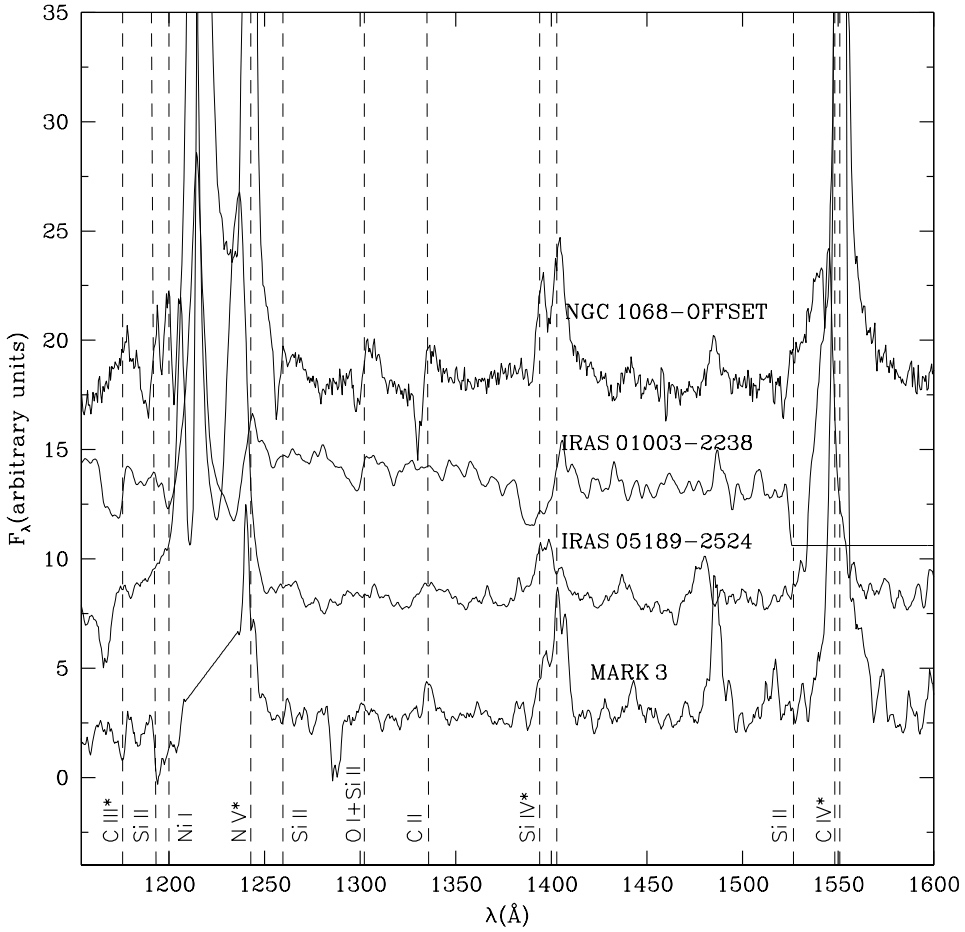

Fig. 7.— Same as Fig. 5 for another 4 spectra.

Table 1. Galaxy sample

Galaxy	RA[a] (hms)	DEC[a] (° ′ ″)	Hubble Type[a]	Activity[a]	Z[a]	Coverage (Å)	References
Q0038+327[b]	00 40 43.5	+32 58 33	–	Sy?	0.1970	1640-3175[b]	–
MARK348	00 48 47.1	+31 57 25	–	HII/WR, Sbrst, Sy2	0.1177	2500-5700	-
IRAS01003-2238	01 02 49.9	-22 21 56	SB(rs)bc	Sy	0.0049	1140-10226	1
NGC613	01 34 18.2	-29 25 07	SA(s)0/a	Sy2	0.0150	6482-7054	2,3
MARK573	01 43 57.8	+02 21 00	(R)SAB(rs)0+	Sy2	0.0172	2900-6867	4
UM146	01 55 22.0	+06 36 43	SA(rs)b	Sy1.9	0.0174	2900-6867	4
NGC788	02 01 06.4	-06 48 56	SA(s)0/a	Sy1, Sy2	0.0136	2900-6867	4
3C67	02 24 12.3	+27 50 12	–	BLRG	0.3102	2900-10226	5
NGC985	02 34 37.8	-08 47 15	SBbc?p(Ring)	Sy1	0.0431	1194-1250	6
NGC1052	02 41 04.8	-08 15 21	E4	LINER, Sy2	0.0049	6295-6867	7,8
NGC1068	02 42 40.7	-00 00 48	(R)SA(rs)b	Sy1, Sy2	0.0038	1140-10266	9,10
NGC1097[d]	02 46 19.0	-30 16 30	(R′_1:)SB(r′l)b	Sy1	0.0042	1140-10266[d]	–
MARK1066	02 59 58.6	+36 49 14	(R)SB(s)0+	Sy2	0.0120	2900-5700	–
NGC1358	03 33 39.7	-05 05 22	SAB(r)0/a	Sy2	0.0134	2900-6867	4
MS0335.4-2618[b]	03 37 36.6	-26 09 08	–	Sy1	0.1230	1150-1740[b]	–
3C109	04 13 40.4	+11 12 14	Opt.var	Ngal, Sy1.8	0.3056	2900-10266	–
3C120	04 33 11.1	+05 21 16	S0,LPQ	BLRG, Sy1	0.0330	2900-10266	–
MARK618[b]	04 36 22.2	-10 22 34	SB(s)b pec	Sy1	0.0355	1640-3175[b]	11
NGC1667	04 48 37.1	-06 19 12	SAB(r)c	Sy2	0.0152	2900-6867	4
3C135	05 14 08.3	+00 56 32	E	BLRG, Sy2	0.1274	5236-10266	12
AKN120[b]	05 16 11.4	-00 08 59	Sb/pec	Sy1	0.0323	1640-3175[b]	11
IRAS05189-2524	05 21 01.3	-25 21 45	pec	Sy2	0.0426	1140-10266	1
NGC1961	05 42 04.8	+69 22 43	SAB(rs)c	LINER	0.0131	6295-6867	–
NGC2110	05 52 11.4	-07 27 22	SAB0-	Sy2	0.0078	6295-6867	13
MARK3	06 15 36.3	+71 02 15	S0	Sy2	0.0135	1140-10266	14,15
NGC2273	06 50 08.7	+60 50 45	SB(r)a	Sy2	0.0062	2900-6867	4
MARK9[b]	07 36 57.0	+58 46 13	S0 pec?	Sy1.5	0.0399	1640-3175[b]	11
MARK78[b]	07 42 41.7	+65 10 37	SB	Sy2	0.0371	1140-7054[b]	16
NGC2787	09 19 18.5	+69 12 12	SB(r)0+	LINER	0.0023	2900-6867	17,18,19,20
NGC2841	09 22 02.6	+50 58 35	SA(r)b	LINER, Sy1	0.0021	8275-8847	–
MARK110	09 25 12.9	+52 17 11	Pair?	Sy1	0.033	1194-1250	–

Table 1—Continued

Galaxy	RA[a] (hms)	DEC[a] (° ′ ″)	Hubble Type[a]	Activity[a]	Z[a]	Coverage (Å)	References
NGC2911	09 33 46.1	+10 09 09	SA(s)0:pec	LINER, Sy	0.0106	6482-7054	–
NGC3031	09 55 33.2	+69 03 55	SA(s)ab	LINER, Sy1.8	-0.0001	8275-8847/6265-6867	21,22
NGC3081	09 59 29.5	-22 49 35	(R_1)SAB(r)0/a	Sy2	0.0079	2900-6867	4
MARK34	10 34 08.6	+60 01 52	Spiral	Sy2	0.0505	2900-5700	–
NGC3227	10 23 30.6	+19 51 54	SAB(s)pec	Sy1.5	0.0039	1140-10266	7,8,23
NGC3393[d]	10 48 23.4	-25 09 43	(R′)SB(s)ab	Sy2	0.0125	2900-6867[d]	24
NGC3516	11 06 47.5	+72 34 07	(R)SB(s)0^0^	Sy1.5	0.0088	1140-5700/6265-6867	24,25
IRAS11058-1131	11 08 20.3	-11 48 12	–	Sy2	0.0548	2900-6867	24
ESO438-G009[d]	11 10 48.0	-28 30 04	(R′_1)SB(rl)ab	Sy1.5	0.0234	1194-1250[d]	26
MCG10.16.111	11 18 57.7	+58 03 24	–	Sy1	0.0279	1194-1250	26
NGC3627	11 20 15.0	+12 59 30	SAB(s)b	LINER, Sy2	0.0024	2900-6867	–
SBS1127+575[b]	11 30 03.6	+57 18 29	–	Sy2	0.0361	1194-1250[b]	26
PG1149-110	11 52 03.5	-11 22 24	–	Sy1	0.0490	1194-1250	26
NGC3982	11 56 28.1	+55 07 31	SAB(r)b	Sy2	0.0037	2900-6867	17,18,19,20
NGC3998	11 57 56.1	+55 27 13	SA(r)0^0^?	LINER, Sy1	0.0035	8275-8847	–
NGC4036	12 01 26.9	+61 53 44	S0-	LINER	0.0048	6295-6867	7,8
3C268.3	12 06 24.7	+64 13 37	–	BLRG	0.3710	5236-10266	12
NGC4138	12 09 29.6	+43 41 17	SA(r)0+	Sy1.9	0.0030	2900-6867	17,18,19,20
IRAS12071-0444	12 09 45.1	-05 01 14	–	Sy2	0.1283	5236-10266	1
NGC4151[d]	12 10 32.6	+39 24 21	(R′)SAB(rs)ab	Sy1.5	0.0033	1140-10266[d]	27 to 33
MARK766	12 18 26.5	+29 48 46	(R′)SB(s)a	Sy1.5	0.0129	1140-3184	–
NGC4258[d]	12 18 57.5	+47 18 14	SAB(s)bc	LINER, Sy1.9	0.0015	8275-8847[d]	2,3
NGC4278	12 20 06.8	+29 16 51	E1-2	LINER, Sy1	0.0022	8275-8847	–
Q1219+047[b]	12 21 37.9	+04 30 26	–	Sy1	0.0940	1194-1250[b]	–
NGC4303	12 21 54.9	+04 28 25	SAB(rs)bc	HIISy2	0.0052	1568-10266	2,3,34
NGC4450	12 28 29.6	+17 05 06	SA(s)ab	LINER, Sy3	0.0065	2900-10266	17,18,19,20
NGC4477	12 30 02.2	+13 38 11	SB(s)0?	Sy2	0.0045	2900-6867	17,18,19,20
M87	12 30 49.4	+12 23 28	E+0-1pec	NLRG, Sy	0.0044	1140-10266	35
NGC4501	12 31 59.2	+14 25 14	SA(rs)b	Sy2	0.0076	2900-6867	17,18,19,20
TON1542	12 32 03.6	+20 09 29	Spiral	Sy1	0.0630	1194-1300	6
NGC4540[b]	12 34 50.8	+15 33 05	SAB(rs)cd	LINER, Sy1	0.0043	2900-5700[b]	–

Table 1—Continued

Galaxy	RA[a] (hms)	DEC[a] (° ′ ″)	Hubble Type[a]	Activity[a]	Z[a]	Coverage (Å)	References
NGC4507	12 35 36.6	-39 54 33	SAB(s)ab	Sy2	0.0118	2900-6867	4
NGC4569	12 36 49.8	+13 09 46	SAB(rs)ab	LINER, Sy	-0.0008	2900-6867	–
NGC4579	12 37 43.6	+11 49 05	SAB(rs)b	LINER, Sy1.9	0.0051	6295-6867	7,8
NGC4594	12 39 59.4	-11 37 23	SA(s)a	LINER, Sy1	0.0034	6482-7054	–
IC3639	12 40 52.8	-36 45 21	SB(rs)bc	Sy2	0.0109	2900-6867	4
NGC4698	12 48 22.9	+08 29 14	SA(s)ab	Sy2	0.0033	2900-6867	17,18,18,20
NGC4736	12 50 53.0	+41 07 14	(R)SA(r)ab	LINER, Sy2	0.0010	6295-6867	–
NGC4826	12 56 43.7	+21 40 52	(R)SA(rs)ab	Sy2	0.0014	2900-6867	–
NGC5005	13 10 56.2	+37 03 33	SAB(rs)bc	Sy2,LINER	0.0032	6482-7054	2,3
IRAS13224-3809[d]	13 25 19.3	-38 24 53	–	Sbrst, NLSy1	0.0667	5236-10266[d]	36,37
NGC5135	13 25 44.0	-29 50 01	SB(l)ab	Sy2	0.0137	2900-5700/6295-6768	4
NGC5194[c]	13 29 52.7	+47 11 43	SA(s)bc pec	HIISy2.5	0.0015	2900-10266[c]	38
NGC5252	13 38 15.9	+04 32 33	S0	Sy1.9	0.0230	2900-5700	24
NGC5283	13 41 05.7	+67 40 20	S0?	Sy2	0.0104	2900-6867	4
TON730	13 43 56.7	+25 38 48	–	Sy1	0.0870	1194-1250	26
NGC5347	13 53 17.8	+33 29 27	(R′)SB(rs)ab	Sy2	0.0078	2900-6867	4
MARK463E	13 56 02.9	+18 22 19	–	Sy1, Sy2	0.0500	2900-5700	-
NGC5427	14 03 26.0	-06 01 51	SA(s)c, pec	Sy2	0.0087	2900-6867	4
Circinus	14 13 09.9	-65 20 21	SA(s)b	Sy2	0.0014	4818-5104	-
NGC5635	14 28 31.7	+27 24 32	S, pec	LINER, Sy3	0.0144	6482-7054	-
NGC5643	14 32 40.8	-44 10 29	SAB(rs)c	Sy2	0.0040	2900-6867	4
MARK817[b]	14 36 22.1	+58 47 39	SBc	Sy1.5	0.0314	2758-2914[b]	39
NGC5695	14 37 22.1	+36 34 04	SBb	Sy2	0.0141	2900-6867	4
NGC5728	14 42 23.9	-17 15 11	(R_1)SAB(r)a	Sy2	0.0093	6295-6867	-
IRAS15206+3342[b]	15 22 38.0	+33 31 36	?	HIISy2	0.1244	1140-10266[b]	1
3C346	16 43 48.6	+17 15 49	E	NLRG, Sy2	0.1620	2900-10266	12
1701+610	17 02 11.1	+60 58 48	–	Sy1.9	0.1649	1140-10266	-
NGC6300	17 16 59.5	-62 49 14	SB(rs)b	Sy2	0.0037	6581-6867	4
PKS1739+184[d]	17 42 06.9	+18 27 21	–	Sy1	0.1860	1140-5700[d]	-
3C405[b]	19 59 28.3	+40 44 02	S?	Radiogal, Sy2	0.0561	2900-5700[b]	40,41
3C382	18 35 02.1	+32 41 50	–	BLRG, Sy1	0.0579	2900-10266	-

Table 1—Continued

Galaxy	RA[a] (hms)	DEC[a] (° ′ ″)	Hubble Type[a]	Activity[a]	Z[a]	Coverage (Å)	References
3C390	18 45 37.6	+09 53 45	–	RadioS	–	2900-5700	-
NGC6951	20 37 14.1	+66 06 20	E+pec?	–	0.0129	6482-7054	2,3
3C445	22 23 49.6	-02 06 12	N galaxy	BLRG, Sy1	0.0562	2900-10266	-
NGC7314	22 35 46.2	-26 03 01	SAB(rs)bc	Sy1.9	0.0048	2900-10266	2,3
AKN564[d]	22 42 39.3	+29 43 31	SB	Sy1.8	0.0247	1140-3184[d]	43,44,45
IC1459	22 57 10.6	-36 27 44	E3	LINER	0.0056	2900-5700	42
NGC7674	23 27 56.7	+08 46 45	SA(r)bc pec	HIISy2	0.0289	2900-5700	-
NGC7682	23 29 03.9	+03 32 00	SA(r)bc pec	HIISy2	0.0289	2900-6867	4

[a]References from NASA/IPAC Extragalactic Database.

[b]Spectra of this galaxy were not extracted due to a poor signal-to-noise ratio in the continuum. Nevertheless, information on the available spectra is also included in the *Mastertable*.

[c]Spectra of this galaxy were not extracted due to the presence of more than one continuum source which we could not identify the brightest one. Information on the available spectra is also included in the *Mastertable*.

[d]Final spectrum of this Seyfert 1 galaxy was obtained with spectra observed in different dates.

Note. — References:1-Farrah et al. (2005), 2-Hughes et al. (2003), 3-Hughes et al. (2005), 4-Pogge et al. (2003), 5-Odea et al. (2003), 6-Penton et al. (2004), 7-Barth et al. (2001a), 8-Barth et al. (2001b), 9-Kraemer et al. (2000b), 10-Cecil et al. (2002), 11-Jenkins et al. (2003), 12-Hutchings et al. (1998), 13-Ferruit et al. (2004), 14-Collins et al. (2005), 15-Ruiz et al. (2001), 16-Whittle et al. (2005), 17-Sarzi et al. (2001), 18-Sarzi et al. (2002), 19-Sarzi et al. (2005), 20-Ho et al. (2002), 21-Chandar, Ford & Tsvetanov (2001a), 22-Chandar, Ford & Tsvetanov (2001b), 23-Crenshaw et al. (2001), 24-Cappetti, Marconi, Macchetto & Axon (2005), 25-Edelson et al. (2000), 26-Bowen et al. (2002), 27-Kaiser et al. (2000), 28-Kraemer et al. (2000a), 29- Nelson et al. (2000), 30-Hutchings et al. (1999), 31-Crenshaw et al. (2000), 32-Hutchings et al. (2002), 33-Kraemer et al. (2001), 34-Colina, González Delgado, Mas-Hesse & Leitherer (2002), 35-Sabra et al. (2003), 36-Leighly (2004), 37-Leighly & Moore (2004), 38-Bradley, Kaiser & Baan (2004), 39-Jenkins et al. (2003), 40-Tadhunter et al. (2003), 41-Bellamy & Tadhunter (2004), 42-Cappellari et al. (2002), 43-Crenshaw et al. (2002), 44-Collier et al. (2001) and 45-Romano et al. (2004).

Table 2. A sample of lines from the *Mastertable*

(1) Galaxy	(2) Rootname	(3) Grating	(4) Aperture ($''$ ^{2})	(5) λ_c (Å)	(6) λ_i (Å)	(7) λ_f (Å)	(8) R	(9) PA (°)	(10) Exp. Time (s)	(11) Name	(12) Scale ($''$ pix^{-1})
MCG10.16.111	o5ew02010	G140M	52x0.2	1222	1194	1250	12200	-86.5063	3900	m1016111-1.234	0.029
	o5ew02020	G140M	52x0.2	1222	1194	1250	12200	-86.5063	3900	m1016111-2.234	0.029
	o5ew02030	G140M	52x0.2	1222	1194	1250	12200	-86.5063	3900	m1016111-3.234	0.029
	o5ew02040	G140M	52x0.2	1222	1194	1250	12200	-86.5063	3900	m1016111-4.234	0.029
	o5ew02050	G140M	52x0.2	1222	1194	1250	12200	-86.5062	3900	m1016111-5.234	0.029
NGC3627	o63n02010	G430L	52x0.2	4300	2900	5700	800	80.0559	2349	n3627-1.80	0.1
	o63n02020	G750M	52x0.2	6581	6295	6867	5980	80.0559	2861	n3627-2.80	0.1
PG1149-110	o5ew05010	G140M	52x0.2	1222	1194	1250	12200	43.6861	2269	p1149-1.44	0.029
	o5ew05020	G140M	52x0.2	1222	1194	1250	12200	43.6861	2899	p1149-2.44	0.029
	o5ew05030	G140M	52x0.2	1222	1194	1250	12200	43.6861	2899	p1149-3.44	0.029
NGC3982	o4e006010	G750M	52X0.2	6581	6295	6867	5980	117.931	900	n3982-1.117	0.05
	o4e006020	G750M	52X0.2	6581	6295	6867	5980	117.931	1197	n3982-2.117	0.05
	o4e006030	G750M	52X0.2	6581	6295	6867	5980	117.931	900	n3982-3.117	0.05
	o4e006040	G430L	52X0.2	4300	2900	5700	800	117.931	900	n3982-4.117	0.05
	o4e006050	G430L	52X0.2	4300	2900	5700	800	117.931	945	n3982-5.117	0.05
IRAS15206+3342	o5f904030	G430L	52x0.2	4300	2900	5700	800	35.3559	780	i1520-3.35	0.05
	o5f904040	G430L	52x0.2	4300	2900	5700	800	35.3559	650	i1520-4.35	0.05
	o5f904050	G750L	52x0.2	7751	5236	10266	790	35.356	624	i1520-5.35	0.05
	o5f904060	G750L	52x0.2	7751	5236	10266	790	35.3559	624	i1520-6.35	0.05
	o5f904070	G750L	52x0.2	7751	5236	10266	790	35.3559	545	i1520-7.35	0.05
	o5f904090	G140L	52x0.2	1425	1140	1730	1190	35.3001	900	i1520-8.35	0.0244

Note. — Columns: (1) the name of the galaxy; (2) the identification of all available STIS spectra for this galaxy in the HST archive, one per line; (3) the grating used in each observation; (4) the slit width of each observation; (5) the central wavelength; (6) the initial wavelength; (7) the final wavelength; (8) the spectral resolution; (9) the slit orientation; (10) the exposure time; (11) The identification of the extracted spectrum from each segment; (12) platescale of the observations.